

Article type: Invited Review

This is the peer reviewed version of the following article: Grazianetti, C., Martella, C. and Molle, A. (2020), The Xenes Generations: A Taxonomy of Epitaxial Single-Element 2D Materials. *Phys. Status Solidi RRL*, 14: 1900439, which has been published in final form at <https://doi.org/10.1002/pssr.201900439>. This article may be used for non-commercial purposes in accordance with Wiley Terms and Conditions for Use of Self-Archived Versions.

The Xenes Generations: a taxonomy of epitaxial single-element two-dimensional materials

*Carlo Grazianetti, Christian Martella, and Alessandro Molle**

Dr. C. Grazianetti, Dr. C. Martella, and Dr. A. Molle
CNR-IMM Agrate Brianza unit, via C. Olivetti 2, Agrate Brianza, I-20864, Italy
E-mail: alessandro.molle@mdm.imm.cnr.it

Keywords: Xenes, two-dimensional, post-graphene, epitaxy, atomically thin

Isolation of graphene is today a milestone in condensed matter physics that paved the way to a new entire class of two-dimensional synthetic materials referred to as Xenes with no analogous bulk layered allotropes. The booming rush to discover first novel and unprecedented materials flew into two generations of Xenes, the first one strictly related to carbon being made of elements of the IV/14 column/group of the periodic table, while the second one includes elements of the adjacent columns. From borophene to tellurene, with rare exceptions, the physics and chemistry of the elements have been rewritten and here reviewed in terms of their fundamental and peculiar properties. A particular attention is paid to the epitaxial methodologies and configurational details aiming at determining key-points for nanotechnology applications of the Xenes afforded by scalability, quality, and stability aspects. Finally, the ongoing efforts to devise and realize applications based on the Xenes are summarized.

Introduction.

In view of incipient challenges on how to move the semiconductor technology forward to a post-silicon era of electronic devices, on 2015 Guy Le Lay stated that “the material to replace

silicon in the electronics industry could, in fact, be silicon itself in the form of silicene".^[1] The statement was originally grounded on the pioneering discovery of a two-dimensional (2D) silicon made framework epitaxially grown on a (111)-terminated silver surface with a quasi-planar structure,^[2] and then captured by the isolation of this atomically thin layer into an operation field effect transistor (FET) with Dirac-like transport.^[3] That was the key to discriminate the so-termed silicene, namely a single atomic layer reproducing a 2D hexagonal lattice, from a silicon-induced decoration of the Ag(111) surface. As such, silicene can be integrally lifted out from its pristine substrate and independently behaves as an active layer in device or as stabilized atomically thin membrane. Another quality of silicene that came up since the original concept of the free-standing lattice is the buckled character of its bonding connections that necessarily stems from an enhanced orbital overlap otherwise too short in a perfectly planar arrangement to guarantee thermodynamic stability.^[4,5] After silicene, a generation of Xenos, silicene-like crystals made of X atoms, has followed up gathering an increasing number of elements X from the group 13 (the boron group) up to the group 16 (the chalcogen group) and passing through the group 15 (pnictogenes group) in the periodic table of elements thus constituting an emerging platforms of novel materials for nanotechnology.^[6] Historically, this evolution can be articulated in two different stages, a first generation limited to the group 14 (the carbon/silicon group) with mutually similar characteristics, issues and a common inspiration towards the quest for a 2D topological insulating state,^[7] and an on-going second generation, out of group 14, where the epitaxial methods were extended to confine down to the 2D level those X elements that seemingly do not possess a stable graphene-like allotrope, not being in a straightforward kinship with carbon as silicon and germanium. A general taxonomy of the Xenos as so far reported is illustrated in **Figure 1** where Xenos are grouped according to the periodic table and key structural properties. The two Xene generations will be briefly described in the following sections. Attention will be then paid to classify the

methodologies for the synthesis of the Xenes, spotlight characteristic aspects of the Xenes, and state application perspectives.

Xenes: First Generation

Xenes were initially inspired by the conceptual option to reduce elements belonging to the group 14 column of the periodic table (out of carbon) in the 2D form of graphene. A historical view on this first generation of Xenes is displayed in **Figure 2** including representative evidences of each single member on its debut. Mastering silicon at the 2D level for a hyper-scaled silicon-based electronics is a technology driver for the Xene development that motivated the initial focus on silicene as a target channel for ultra-thin body transistors owing to silicon ubiquity in microelectronics.^[8] In a later stage, spanning elements in the group 14 column was basically inspired by the ambition to make a 2D elementary crystal with non-trivial topology, namely a 2D topological insulator at room temperature, eventually aiming at topological quantum electronics.^[7]

Silicene.

Silicene was first synthesized as epitaxial layer on Ag(111) substrates^[2,9] therein displaying a multiphase character,^[10] then as a segregated layer on ZrB₂/Si(111) artificial substrates.^[11] Starting from the single layer, multilayer silicene was lately proven through an island growth mode on Ag(111).^[12–14] The quest for alternative substrates lead many research groups to bring evidences of silicene growth on other (111)-terminated metal substrates, like iridium, gold, and lead,^[15–17] layered materials such as MoS₂ and graphite,^[18,19] and other lattice-matched compounds like ZrC and c-Al₂O₃.^[20,21] Alternatively, silicene was also identified as a surface reconstruction in MoSi₂ substrates or as intercalated plane in layered CaSi₂ compounds.^[22–24] In the latter fashion, silicene was isolated as functionalized layer inside Zintl phase crystals

such as SrSi_2 , GdSi_2 , and EuSi_2 aiming at 2D ferromagnetism,^[25–27] and intercalated in between a pre-grown graphene layer and $\text{Ag}(111)$.^[28] While most of the evidences about silicene epitaxy are concerned with metallic substrates, $c\text{-Al}_2\text{O}_3$ was currently reported to be the only insulating substrate supporting silicene based on theoretical and experimental facts.^[21] Parallel to substrate selection is the effort to handle silicene in a process flow aiming at applications. A breakthrough in this sense dates back to the epitaxy of silicene on epi- $\text{Ag}(111)$ -on-mica substrates (instead of silver monocrystals) enabling delamination of encapsulated silicene sheet readily integrable into transistor device structures.^[3,14] Modulated carrier conduction was also observed at the interface between silicene and MoS_2 although this configuration was debated owing to possible intercalation of silicon inside the MoS_2 planes.^[29–31]

Germanene.

Germanene quickly followed up from the debut of silicene as epitaxial crystal on substrate. Similar to silicene, (111)-terminated metal surface of aluminum, gold, platinum, copper, antimony, and silver proved to be good templates for germanene epitaxy.^[32–37] Silver has been also used as buffer layer for germanene epitaxy through segregation.^[38] Germanene formation was demonstrated on Ge_2Pt crystals after deposition of platinum on $\text{Ge}(110)$ and subsequent high-temperature annealing.^[39] Unlike silicene, germanene was shown to grow on hexagonal AlN on $\text{Ag}(111)$.^[40] Growth of small germanene domains was also reported on layered substrates like MoS_2 and graphite.^[41,42] Similarly to silicene, multilayer germanene has been reported as well.^[43]

Stanene and plumbene.

2D tin (equivalently termed stanene, stannene or tinene) was considered to be the more promising candidate to access a quantum spin Hall state displaying a theoretically sizeable energy spin-orbit-induced gap (100 meV possibly extendable by functionalization).^[44] At the moment, due to the hexagonal symmetry of (111)-surfaces, several achievements about 2D tin growth lead to the realization of (metallic) stanene on Bi_2Te_3 , copper, InSb , antimony, and silver,

the two latter cases offering common templates with silicene and germanene.^[45-49] It should be also noticed that a stanene-like configuration was also approached by epitaxial thinning tin film with a slightly distorted α -phase (reckoned as the three-dimensional (3D) counterpart of stanene) on nearly matched InSb(111) substrates therein displaying Dirac-like electronic bands in the multilayer regime.^[50] Very recently, 2D lead, termed plumbene, was reported as arising from the segregation of lead atoms from a $\text{Pd}_{1-x}\text{Pb}_x(111)$ substrate.^[51]

Xenes: Second Generation.

Inspired by the results achieved in the group 14 elements and by the booming interest related to non-graphene elementary 2D crystals like black phosphorus (BP) nanosheets,^[52,53] soon research groups around the world started wondering whether forcing atoms to arrange into 2D sheets was possible even for those elements of the periodic table around the 14 column (say X elements), from the lighter boron to the heavier tellurium. This second generation of Xenes was mostly synthesized by epitaxy on substrates starting from favorable epitaxial relationships with the substrate as for silicene or similar, but the majority of the cases took benefits from the intrinsic layered structure or hexagonal character of some stable bulk allotrope (see for instance, the case of 2D pnictogens as reviewed in Ref.^[54]). As for the first generation, a historical view on the second generation of Xenes is given in **Figure 3** including more representative results for each member at its debut. According to **Figure 1**, in the following we list the members of the second generation of Xenes following the columnar group of the periodic table.

Group 13 Xenes

Borophene. Stepping out from the group 14 column in the periodic table, the first element to be considered as constituent of a new 2D monoelemental crystal is boron to form the so-called borophene. Borophene is expected to be lightest 2D metal, despite bulk boron being a semiconductor, for most structures characterized by anisotropy and polymorphism.^[55,56]

Although metallic in character, Dirac fermions have been observed in borophene as well as active Raman modes.^[57,58] Like silicene, borophene epitaxy was initially reported on Ag(111), then successfully shifted on Au(111) and Cu(111), according to the theoretical predictions.^[55,56,59,60] In light of its metallicity, the potential applications deemed to exploit the borophene properties are related to plasmonics, superconductivity, and transparent electrodes for flexible electronics.

Gallenene. 2D gallium (termed gallenene) was very recently obtained by means of a solid–melt exfoliation process on SiO₂/Si substrate and by means of epitaxy on Si(111) substrate.^[61,62] In the former case, gallenene presents two distinct crystallographic orientations along twin directions of the bulk α -gallium. It shows low thermal conductivity and strong chemical interaction with the substrate, confirmed both theoretically and experimentally.^[61] In the latter case, *in situ* low-temperature scanning tunneling microscopy (STM) and spectroscopy (STS) reveal that the epitaxial growth of gallenene on Si(111) proceeds starting with a buffer layer, showing a $4\times\sqrt{13}$ reconstruction of the substrate lattice, and then a second layer characterized by a hexagonal honeycomb structure. The STS measurements confirmed the theoretical prediction of the gallenene metallic character.

Group 15 Xenos.

Elements of the group 15 in the periodic table (known as pnictogens) can generally exhibit two allotropic forms in their stable bulk structures, namely the orthorhombic and the rhombohedral forms. When reduced to the 2D level, the former one is the crystallographic structure of the well-known BP and results in van der Waals layered solids eventually leading to a puckered atomic layer (as in case of phosphorene, a single BP layer), whereas the latter one recasts as a buckled atomic sheet nearly similar to the free-standing form of silicene and other group 14 Xenos (see Figure 1).

(Blue) Phosphorene. Paralleled with the BP (occasionally called phosphorene in its ultra-thin form),^[52] phosphorus was epitaxially synthesized as a 2D lattice on Au(111) surface thus

resulting in a reconstructed phase of the single layer of the new allotropic phase of phosphorus, *i.e.* blue phosphorus for the theoretically expected energy gap in excess of 2 eV.^[63] Conventionally termed blue phosphorene is a true epitaxial material because it grows by deposition of P₄ molecules on Au(111) surface. Epitaxial phosphorene on Au(111) has been reported to show a single phase covering the whole substrate due to self-limited growth and a semiconducting behavior with a reported bandgap of ~1 eV.^[64–68] Despite the metal substrate, such a bandgap value makes it appealing as 2D materials for electronics although no evidence of device has been so far reported. However, recently the first steps towards epitaxial phosphorene integration were initiated by embedding it in between a thin gold film and the Al₂O₃ capping layer, thus mimicking the configuration that successfully enabled silicene integration.^[69]

Antimonene. The first experimental realizations of 2D antimony, namely antimonene, were obtained by micromechanical and liquid exfoliation.^[70,71] So far, the epitaxial growth of antimonene has been reported on Bi₂Te₃ and Sb₂Te₃, PdTe₂, Ge(111), Ag(111), Pb(111), Cu(111) and Cu(110).^[72–77] Furthermore, van der Waals epitaxy of antimonene was successfully obtained on graphene^[78] and mica substrates,^[79] together with the first experimental realization of α -antimonene on WTe₂ substrate, therein sharing the same puckered structure with BP.^[80] Theoretical works predict a variety of appealing physical-chemical properties of antimonene including tunable electronic bandgap, low thermal conductance and electrical resistivity,^[81] and nontrivial topological features.^[54,82] These findings, together with an extremely high environmental stability,^[70] make antimonene one of the most promising second-generation Xene in a wealth of technological applications, including photonics,^[83] electronics,^[79,84,85] and sodium-ion batteries.^[86]

Arsenene. Despite the large number of theoretical works devoted to unveil the electronic properties of 2D arsenic, including indirect-to-direct bandgap transition,^[87] high carrier

mobility,^[85] and non-trivial topological states,^[88] the experimental reports on the arsenene synthesis are so far limited to a few evidences based on liquid phase exfoliation.^[89]

Bismuthene. All along the fashion of stanene, due to the high-atomic number, bismuth showed up as a promising element to incorporate non-trivial topological properties such as conduction channels at the edges that are inherently protected against certain types of scattering.^[90] With this concept in mind, bismuthene domains were grown on a SiC(0001) surface that feature edged-localized electronic states as candidates of a one-dimensional topologically protected edge states.^[91]

Group 16 Xenos

Selenene and Tellurene. Selenium and Tellurium, belonging to the chalcogens family (group 16 in the periodic table), share the same crystal structure in which atoms are covalently connected in a spiral chain along the c-axis (see **Figure 1**). Due to this anisotropic chain-like arrangement, they tend to form one-dimensional (1D) structures like nanowires or nanotubes.^[92] Nevertheless, they were both recently reduced to the 2D Xene form on substrates, obtaining selenene and tellurene nanosheets. Selenene was synthesized by physical vapor deposition (PVD) on Si (111) substrates and investigated by angle-resolved Raman investigations showing a strong in-plane anisotropy.^[93] Moreover, selenene was tested as active material in a back-gated FET showing p-type carrier mobility and promising switching characteristics.^[93] Hexagonal 2D domains of tellurene were for the first time grown by van der Waals epitaxy on flexible mica substrate.^[94] Subsequently, liquid phase exfoliation,^[95] solution-based growth^[96] and van der Waals epitaxy on graphene^[97] were successfully used for the synthesis of tellurene nanosheets that have shown to exhibit anisotropic and thickness-dependent electrical properties,^[96] photoelectric response,^[94,95] and distinctive magneto-transport behavior.^[92]

Epitaxial methodologies, commensurate substrates, and driving force for the Xenos growth

Epitaxy is the more popular way to synthesize Xenes so far. Epitaxy is a bottom-up approach to grow a crystalline film on a crystalline substrate with the same normal orientation. A variant, that came up with the advent of 2D materials, is the van der Waals epitaxy where the growth is no longer mediated by the substrate surface (*e.g.* by dangling bond) but takes place under a van der Waals driving force with no significant covalent bonds or orbital overlap occurring.^[98] While it turns out to be mandatory for most of the Xenes, there are some cases of Xene synthesis where the epitaxial relationship may not be needed such as the vapor transport deposition of tellurene on mica,^[94] the solid-melt exfoliation of gallenene,^[61] or the liquid exfoliation of borophene, antimonene, arsenene, and tellurene nanosheets.^[71,89,95,99] Despite these growth methods are relatively cheaper, molecular beam epitaxy ensures to fulfill some requirements, *e.g.* scalability (see next section), that are mandatory for nanotechnology applications. Therefore, here we will focus on epitaxial methodologies. These ones can be articulated as follows (see **Figure 4**): 1) Epitaxy by deposition (Figure 4a). It consists of the condensation of the melted X species onto a host substrate in ultra-high vacuum conditions. This is the more extensively used approach to the growth of Xenes on substrate nearly including all the possible X species as detailed above.^[100,101] 2) Epitaxy by segregation (Figure 4b). This is the case of X element interdiffusion from a substrate towards the surface with subsequent arrangement in a honeycomb-like fashion as reported for silicene on ZrB₂, germanene on Ag(111), borophene on Au(111), and plumbene on PdPb alloy.^[38,51,59,102] For the particular case of silicene, the silicon interdiffusion sets in through a commensurate buffer layer (grown on purpose onto bulk silicon acting as silicon reservoir), *e.g.* ZrB₂, that accommodates the silicene layer on top.^[102] This methodology could be effective in decoupling the Xene layer from the substrate, *e.g.* by engineering insulating buffer layers. 3) Epitaxy by intercalation (Figure 4c). Similar to deposition in item 1), X atoms are evaporated from a nearby source onto a matrix crystal that is either permeable to X atom, crossing through so as to form an Xene sheet in contact with a commensurate substrate (this is the case of silicene intercalated in between graphene and

Ag(111), **Figure 4c** top),^[28] or prone to form a Zintl crystal film where the Xene is a constitutive block in between two other metallic planes (this is the case of silicene planes incorporated in Zintl silicide structure of the MSi_2 form, where M is a rare-earth like europium, strontium, and gadolinium, **Figure 4c** bottom).^[25-27]

There are two general concepts driving the Xene epitaxy which depend on the elemental species X and/or their crystal bulk structure, namely epitaxy on commensurate substrates and growth of stable allotropes. The former one is basically related to substrate as commensurate template for the Xene lattice formation, and generally applies to Xenenes that are not inherently stable in Nature in their freestanding form, namely $X=B, Si, Ge,$ and Pb . As an exception to this rule, the growth of epitaxial (blue) phosphorene single layer belongs to this category even if its rhombohedral structure corresponds to stable allotrope in predicted bulk. This is due to the fact that epitaxial phosphorene grows on Au(111) by virtue of a catalytic surface reaction and is hence self-limited to a single layer.^[65] Generally speaking, we take the first Xene generation, in particular silicene, as a case in point. Bulk silicon is intrinsically arranged in a face-centered diamond-like cubic structure with each atom having a tetrahedral coordination while no layered crystal structure, say silicite, is permitted. Nonetheless a 2D silicon with a honeycomb crystal symmetry is made energetically possible only if a vertical distortion of atomic bonding takes place with a regular periodicity in a conceptualized free-standing lattice (hereafter termed ideal silicene). This buckled lattice is the energetically permitted form for silicene to be epitaxially landed on substrates. Incidentally, buckling might act as an additional degree of freedom when manipulating artificial crystal lattices like those of the Xenenes in order to modify their properties, *e.g.* opening a bandgap by means of an electric field or by adsorption of foreign chemical species.^[103,104] Severe constraints apply to this kind of epitaxy. One is the commensurability relationship between the ideal silicene and the substrate surface eventually giving rise to the multiphase character of the Xene.^[10,105,106] Another condition is the carefully tailored growth parametrization resulting in a kinetically driven self-assembly of the silicene. A first

consequence in this respect is the nucleation of silicene seeds in a sub-monolayer growth regime (see **Figure 4d**) eventually leading to a 2D structured domains with the growth coming along (see **Figure 4e**). A second implication is the phase diagram of silicene displaying several commensurate silicene structures (namely phases) as a function of the growth temperature and the deposition flux or coverage governing the adatom diffusivity and the chemical potential, respectively,^[106] up to the multilayer regime.^[12,14]

On the other hand, a different derivation of Xene epitaxy stems from the dimensional reduction of a stable bulk phase. Within this number are group 15 and 16 elements herein including recently reported antimonene, selenene, and tellurene (but not epitaxial phosphorene as previously argued while the case of bismuthene is still under survey). With a similar concept in mind, stanene can be derived seemingly by reducing the thickness of slightly distorted α -Sn ultra-thin film as grown on InSb(111) substrates down to the 2D state.^[47,50] Owing to the intrinsic hexagonal symmetry of the crystal lattice, this kind of Xenenes can be epitaxially grown in the 2D form with no compulsory commensurability constraints as in case of group 14 Xenenes. Substrates play a pivotal role in the epitaxy of the majority of Xenenes on commensurate substrates. Even if the atomic details (*e.g.* buckling, structural phases) are dictated by the coincidence with the substrate surface symmetry, in some cases this necessary condition is however not sufficient to preserve the original electronic character of the Xene when supported by the substrate. In this framework a paradigmatic example is silicene on Ag(111) where coupling with the substrate results in a metallic character of the overall silicene-substrate system as demonstrated by a comparative carrier dynamics study of silicene-on-Ag(111) with respect to bulk silicon and lone Ag(111),^[107] see **Figure 4f**. However, in general, the role of substrate can be carefully taken into account either for determining the peculiar characteristics of the Xenenes or for stabilizing new Xenenes phases. Stanene overall electronic character has been proven to switch from metallic to quantum spin Hall insulator by changing the supporting template from Bi₂Te₃(111) to Cu(111) via buckling engineering of the stanene lattice.^[46,48] The

borophene polymorphs can be tuned by different metallic substrates ranging from a flatter structure on silver, copper and gold to the one with a significant off-plane buckling that is favored on gold, because of the different borophene's electron affinity with the substrates.^[55,56,59,60] Similarly, a change in the buckled configuration of epitaxial antimonene is observed as a function of the crystal orientation of the copper substrates,^[76] thus resulting in a strain-induced tunability of the antimonene electronic bandgap. Finally, a different example about the role of substrates is related to the catalytic role of Au(111) surface in dissociating the P₄ molecules in the evaporation flux and then promoting the self-limited growth of the epitaxial phosphorene.^[65,67] Nonetheless, opposed to the proximity effect of the silver substrates in the “metallization” of silicene, such a catalytic activity has little influence in the semiconducting character of the epitaxial phosphorene.

Scalability, quality, and stability

Epitaxial methodologies usually yield a large-scale extension of Xenes over macroscopic domain size (actually limited by the atomic terrace width on the host surface) in most of the reported cases where Xenes uniformly wet the substrate surface with limited 3D cluster formation. Reported examples of extended Xene layer includes silicene on Ag(111),^[2] germanene on Al(111),^[33] epitaxial phosphorene on Au(111),^[67] and so on. It may occur that owing to the high X atom diffusivity on specific surface or site-selective coalescence, Xene may grow as islands with nanoscaled size, see for instance the case of silicene on graphite or germanene islands on Cu(111).^[19,108] Nonetheless, large-scale production shows up as a major benefit of epitaxial Xenes compared to other 2D players where single-layer scalability is an issue and often promising 2D materials like BP, actually recast as microscaled flakes with limited surface coverage. On the other hand, large Xene coverage is dictated by the recovery of an atomically flat support surface as in case of (111)-terminated metal substrates (see the example of borophene on copper of **Figure 5a**).

Although Xenes can be scaled up to a macroscopic size, epitaxy on substrates often results in a polycrystalline 2D growth characterized by the coexistence of 2D grains differently rotated with respect to the substrate with grain boundaries disconnecting adjacent domains.^[60,105] A scenario of this kind originally affected graphene as well,^[109] therefore, on the same line, further studies focused on the isolation of the single Xene phases, by carefully tailoring the growth parameters, are highly demanded.^[106] The overall improvement of the crystalline quality of the Xene would result in reliable and viable processing integration schemes as well as in better device performances.^[3,14] Aiming at an improved quality of the synthesized Xenes by epitaxy on substrates, the study of (point and/or line) defects is of primary importance and mostly carried out by scanning probe microscopy tools, *e.g.* STM and STS, corroborated by theoretical modeling thus allowing for an atomic scale characterization of defects and growth mechanisms (see **Figure 5b** for an example reported on antimonene on copper).^[76,110,111]

Stability is another key-issue for technology exploitation of Xenes. In particular, Xenes resulting from the substrate commensuration, that inherently presents a mixed sp^2/sp^3 bonding in their buckled metastable structure, are subject to degradation in ambient condition leading to overall oxidation. For instance, in the silicene case, the mixed sp^2/sp^3 bonding hybridization shows up in the low buckled honeycomb structure that is stable, *i.e.* it has no imaginary phonon modes in the Brillouin zone, whereas a single sheet of silicon with sp^3 structure is not.^[5] It is not surprising find out such differences between carbon and silicon/germanium considering that sp^3 carbon, *e.g.* diamond, is not favored at room temperature and ambient pressure while silicon and germanium naturally arrange this way. Chemically, silicene, borophene, stanene, and epitaxial phosphorene have been observed to oxidize when exposed to air, even if oxidation is shown to be limited when exposed to pure O₂ under ultrahigh vacuum conditions.^[48,55,56,112,113] The different chemical reactivity and degradation mechanism is still unclear and is likely that the oxidation is favored by other atmospheric species like H₂O. Similarly, the reactivity of tellurene and antimonene when exposed to ambient condition is still under investigation, even

though a robust chemical stability has been observed in the multi-layer regime over months of exposure by monitoring their structural and electronic transport properties.^[80,96] Stability issues can be overcome by applying encapsulation schemes like sequential Al₂O₃ layer capping after the Xene growth, as reported for the silicene on c-Al₂O₃ in **Figure 5c**.^[21,112] This encapsulation layer acts as a stabilizer for the Xene structure, and allows for subsequent *ex situ* diagnostic with no apparent materials degradation. Outside the growth environment, Raman and optical spectroscopies are effective probes to check the integrity of the Xenenes layers after encapsulation,^[21,114] and then monitor the materials quality throughout a complete process flow (*e.g.* device integration).

Perspectives of applications.

Graphene technology is by far more advanced than the Xene one. Nonetheless, a common aspect relies on two available approaches to the materials production and handling, namely *direct growth on substrate* vs. *growth and transfer*. The former case is confined to the configuration in which the substrate concomitantly hosts the Xene and enables its integration into devices. The more favorable configuration in this sense is the Xene-on-insulator for its subsequent integration into electronic and photonic device structures. So far, a few promising cases have been reported, they include antimonene and tellurene grown on flexible mica substrate and tested respectively as transparent conductive electrodes and active material for photodetection,^[79,94] silicene grown on optical transparent c-Al₂O₃ which enables silicene application in photonics and plasmonics due to its Dirac-like optical conductivity.^[21] On the contrary, Xenenes on metals are more readily addressed to delamination from substrate and transfer to a device platform with possible process-induced modifications or degradation of their inherent structure. This approach was successfully used to fabricate silicene transistors (**Figure 6b**).^[3,14] Encapsulated Xene sheets can be isolated and detected by means of Raman spectroscopy thus making transfer to a secondary substrate possible. However, stability issues

must be faced whenever silicene or other similar Xenes-on-metals are deprived from their native substrates. Several encapsulation stages should be needed to prevent the reactivity on both faces of the Xenes. Degradation is significantly mitigated when considering the multilayer Xene. For instance, in silicene multilayer only the upmost layer is affected by oxidation.^[12] When properly transferred, Xenes can be operated as electronically active materials. Apart from the above-mentioned silicene transistors, concrete cases are those of tellurene and selenene multilayers, which share promising electronic transport features when integrated into functional FETs, phototransistors, and photodetectors (Figure 6a).^[93,96,115] A perspective in this sense is also appealing for 2D epitaxial pnictogens like phosphorene, arsenene, and antimonene as they present a sizeable (direct) energy gap allowing for (opto)electronic operations.^[85] In particular, all of them are appealing as 2D semiconducting single layer for digital devices. Antimonene as extreme case of elementary antimony can be also listed among the possible options to realize a monoelemental non-volatile memory based on a power-induced phase change mechanism.^[84] Overall, Xenes are expected to reduce power consumption in device operations by greatly lowering the applied voltages and by taking benefit from their atomic thickness in the charge flow (*e.g.* minimization of short channel effects). Nonetheless, performances in device are yet to be tested in figure of merits to be benchmarked with other emerging options either in the 2D field or outside. Aiming at nearly zero energy devices, a paradigm shift in the basic mechanism of nanoelectronics devices can come from heavier Xenes like stanene, bismuthene, and plumbene as there are promising candidates to develop so-called topological FETs (**Figure 6c**). In this framework the topological state (nontrivial topology with dissipationless edge conduction vs. trivial topology with insulating behavior) would work out as a logic bit instead of the inversion-depletion-accumulation of the space charge region in a conventional semiconductor.^[7,116] Currently, only 2D ditelluride like WTe₂ proved topological transport whereas a clear topological hallmark in the transport features is still missing among heavier Xenes.^[117,118] The exploitation of these features on the as-grown stanene, bismuthene, and

plumbene still requires to develop appropriate device architectures that has yet to come in order to gain benefit from their expected topologically protected transport. It should be anyway noted that few layers stanene was unexpectedly observed to undergo a superconducting transition below 1.2 K.^[119]

Finally, Xene exploitation in energy production is envisioned thanks to the robust thermoelectric figure of merit predicted for antimonene, tellurene and selenene,^[81,120] together with the high ion storage performance shown by antimonene-graphene heterostructures in view of innovative sodium ion batteries.^[86]

Conclusions

Since 2012, the year of the debut of silicene as first epitaxial Xene beyond graphene, a flourishing of discoveries has followed up throughout more and more elements of the periodic table recasting as 2D epitaxial Xenos. Not only group 14 elements (namely elements belonging to the group of carbon and silicon) were forced to the 2D level by making use of commensurate templates, but other surrounding elements proved to assume an ultra-scaled dimensional form. Here, epitaxial materials were taken into account since they are intrinsically scalable with potential for device integration. In this respect, the structural quality and the stabilization are necessary steps to enable epitaxial Xenos for further processing. Provided that viable processing schemes are developed, Xenos may address a number of applications ranging from nano- and micro-electronics herein including low power and/or high performance electronics, flexible electronics, or new forefront in quantum electronics based on non-trivial topological features, light-matter interaction implying optoelectronics, photonics, and plasmonics with focus on THz devices, and energy applications including new building blocks for solar cells, thermoelectric modules, and batteries. In addition, with the same surprise manifested by Soucheng Zhang (who first forecast the topological character of stanene at room temperature) in face of the evidence of superconductivity in few-layer stanene while conversely looking for the quantum spin Hall

by the low-temperature magneto-transport technique,^[119] we can expect that room for exploration of unexpected or exotic effects is still wide open for this kind of nanomaterials.

Acknowledgements

The Authors acknowledge EU funding from the H2020 research and innovation programme under the ERC-COG 2017 grant no. 772261 “XFab”.

Received: ((will be filled in by the editorial staff))
Revised: ((will be filled in by the editorial staff))
Published online: ((will be filled in by the editorial staff))

References

- [1] G. Le Lay, *Nat. Nanotechnol.* **2015**, *10*, 202.
- [2] P. Vogt, P. De Padova, C. Quaresima, J. Avila, E. Frantzeskakis, M. C. Asensio, A. Resta, B. Ealet, G. Le Lay, *Phys. Rev. Lett.* **2012**, *108*, 155501.
- [3] L. Tao, E. Cinquanta, D. Chiappe, C. Grazianetti, M. Fanciulli, M. Dubey, A. Molle, D. Akinwande, *Nat. Nanotechnol.* **2015**, *10*, 227.
- [4] K. Takeda, K. Shiraishi, *Phys. Rev. B* **1994**, *50*, 14916.
- [5] S. Cahangirov, M. Topsakal, E. Aktürk, H. Şahin, S. Ciraci, *Phys. Rev. Lett.* **2009**, *102*, 236804.
- [6] M. Houssa, A. Dimoulas, A. Molle, A. Dimoulas, A. Molle, *2D Materials for Nanoelectronics*, CRC Press, **2016**.
- [7] A. Molle, J. Goldberger, M. Houssa, Y. Xu, S. C. Zhang, D. Akinwande, *Nat. Mater.* **2017**, *16*, 163.
- [8] S. Salahuddin, K. Ni, S. Datta, *Nat. Electron.* **2018**, *1*, 442.
- [9] C.-L. Lin, R. Arafune, K. Kawahara, N. Tsukahara, E. Minamitani, Y. Kim, N. Takagi, M. Kawai, *Appl. Phys. Express* **2012**, *5*, 045802.
- [10] D. Chiappe, C. Grazianetti, G. Tallarida, M. Fanciulli, A. Molle, *Adv. Mater.* **2012**, *24*,

5088.

- [11] A. Fleurence, R. Friedlein, T. Ozaki, H. Kawai, Y. Wang, Y. Yamada-Takamura, *Phys. Rev. Lett.* **2012**, *108*, 245501.
- [12] P. De Padova, C. Ottaviani, C. Quaresima, B. Olivieri, P. Imperatori, E. Salomon, T. Angot, L. Quagliano, C. Romano, A. Vona, M. Muniz-Miranda, A. Generosi, B. Paci, G. Le Lay, *2D Mater.* **2014**, *1*, 021003.
- [13] P. Vogt, P. Capiod, M. Berthe, A. Resta, P. De Padova, T. Bruhn, G. Le Lay, B. Grandidier, *Appl. Phys. Lett.* **2014**, *104*, 021602.
- [14] C. Grazianetti, E. Cinquanta, L. Tao, P. De Padova, C. Quaresima, C. Ottaviani, D. Akinwande, A. Molle, *ACS Nano* **2017**, *11*, DOI 10.1021/acsnano.7b00762.
- [15] L. Meng, Y. L. Wang, L. Z. Zhang, S. X. Du, R. T. Wu, L. F. Li, Y. Zhang, G. Li, H. T. Zhou, W. A. Hofer, H.-J. J. Gao, *Nano Lett.* **2013**, *13*, 685.
- [16] S. Sadeddine, H. Enriquez, A. Bendounan, P. Kumar Das, I. Vobornik, A. Kara, A. J. Mayne, F. Sirotti, G. Dujardin, H. Oughaddou, *Sci. Rep.* **2017**, *7*, 44400.
- [17] A. Stępniań-Dybala, M. Krawiec, *J. Phys. Chem. C* **2019**, *123*, 17019.
- [18] D. Chiappe, E. Scalise, E. Cinquanta, C. Grazianetti, B. van den Broek, M. Fanciulli, M. Houssa, A. Molle, *Adv. Mater.* **2014**, *26*, 2096.
- [19] M. De Crescenzi, I. Berbezier, M. Scarselli, P. Castrucci, M. Abbarchi, A. Ronda, F. Jardali, J. Park, H. Vach, *ACS Nano* **2016**, *10*, 11163.
- [20] T. Aizawa, S. Suehara, S. Otani, *J. Phys. Chem. C* **2014**, *118*, 23049.
- [21] C. Grazianetti, S. De Rosa, C. Martella, P. Targa, D. Codegoni, P. Gori, O. Pulci, A. Molle, S. Lupi, *Nano Lett.* **2018**, *18*, 7124.
- [22] E. Noguchi, K. Sugawara, R. Yaokawa, T. Hitosugi, H. Nakano, T. Takahashi, *Adv. Mater.* **2015**, *27*, 856.
- [23] R. Yaokawa, T. Ohsuna, T. Morishita, Y. Hayasaka, M. J. S. Spencer, H. Nakano, *Nat. Commun.* **2016**, *7*, 10657.

- [24] C. Volders, E. Monazami, G. Ramalingam, P. Reinke, *Nano Lett.* **2017**, *17*, 299.
- [25] A. M. Tokmachev, D. V. Averyanov, I. A. Karateev, O. E. Parfenov, O. A. Kondratev, A. N. Taldenkov, V. G. Storchak, *Adv. Funct. Mater.* **2017**, *27*, 1606603.
- [26] A. M. Tokmachev, D. V. Averyanov, O. E. Parfenov, A. N. Taldenkov, I. A. Karateev, I. S. Sokolov, O. A. Kondratev, V. G. Storchak, *Nat. Commun.* **2018**, *9*, 1672.
- [27] A. M. Tokmachev, D. V. Averyanov, I. A. Karateev, O. E. Parfenov, A. L. Vasiliev, S. N. Yakunin, V. G. Storchak, *Nanoscale* **2016**, *8*, 16229.
- [28] G. Li, L. Zhang, W. Xu, J. Pan, S. Song, Y. Zhang, H. Zhou, Y. Wang, L. Bao, Y.-Y. Zhang, S. Du, M. Ouyang, S. T. Pantelides, H.-J. Gao, *Adv. Mater.* **2018**, *30*, 1804650.
- [29] A. Molle, A. Lamperti, D. Rotta, M. Fanciulli, E. Cinquanta, C. Grazianetti, *Adv. Mater. Interfaces* **2016**, *3*, 1500619.
- [30] R. van Bremen, Q. Yao, S. Banerjee, D. Cakir, N. Oncel, H. J. W. Zandvliet, *Beilstein J. Nanotechnol.* **2017**, *8*, 1952.
- [31] W. Peng, T. Xu, P. Diener, L. Biadala, M. Berthe, X. Pi, Y. Borensztein, A. Curcella, R. Bernard, G. Prévot, B. Grandidier, *ACS Nano* **2018**, *12*, 4754.
- [32] M. E. Dávila, L. Xian, S. Cahangirov, A. Rubio, G. Le Lay, *New J. Phys.* **2014**, *16*, 095002.
- [33] M. Derivaz, D. Dentel, R. Stephan, M. C. Hanf, A. Mehdaoui, P. Sonnet, C. Pirri, *Nano Lett.* **2015**, *15*, 2510.
- [34] J. Gou, Q. Zhong, S. Sheng, W. Li, P. Cheng, H. Li, L. Chen, K. Wu, *2D Mater.* **2016**, *3*, 045005.
- [35] L. Li, S. Lu, J. Pan, Z. Qin, Y. Wang, Y. Wang, G. Cao, S. Du, H.-J. Gao, *Adv. Mater.* **2014**, *26*, 4820.
- [36] Z. Qin, J. Pan, S. Lu, Y. Shao, Y. Wang, S. Du, H.-J. Gao, G. Cao, *Adv. Mater.* **2017**, *29*, 1606046.
- [37] C.-H. Lin, A. Huang, W. W. Pai, W.-C. Chen, T.-Y. Chen, T.-R. Chang, R. Yukawa,

- C.-M. Cheng, C.-Y. Mou, I. Matsuda, T.-C. Chiang, H.-T. Jeng, S.-J. Tang, *Phys. Rev. Mater.* **2018**, *2*, 024003.
- [38] J. Yuhara, H. Shimazu, K. Ito, A. Ohta, M. Araidai, M. Kurosawa, M. Nakatake, G. Le Lay, *ACS Nano* **2018**, *12*, 11632.
- [39] P. Bampoulis, L. Zhang, A. Safaei, R. van Gastel, B. Poelsema, H. J. W. Zandvliet, *J. Phys. Condens. Matter* **2014**, *26*, 442001.
- [40] F. d'Acapito, S. Torrenco, E. Xenogiannopoulou, P. Tsipas, J. Marquez Velasco, D. Tsoutsou, A. Dimoulas, *J. Phys. Condens. Matter* **2016**, *28*, 045002.
- [41] L. Zhang, P. Bampoulis, A. N. Rudenko, Q. Yao, A. van Houselt, B. Poelsema, M. I. Katsnelson, H. J. W. Zandvliet, *Phys. Rev. Lett.* **2016**, *116*, 256804.
- [42] L. Persichetti, F. Jardali, H. Vach, A. Sgarlata, I. Berbezier, M. De Crescenzi, A. Balzarotti, *J. Phys. Chem. Lett.* **2016**, *7*, 3246.
- [43] M. E. Dávila, G. Le Lay, *Sci. Rep.* **2016**, *6*, 20714.
- [44] Y. Xu, B. Yan, H.-J. Zhang, J. Wang, G. Xu, P. Tang, W. Duan, S.-C. Zhang, *Phys. Rev. Lett.* **2013**, *111*, 136804.
- [45] J. Yuhara, Y. Fujii, K. Nishino, N. Isobe, M. Nakatake, L. Xian, A. Rubio, G. Le Lay, *2D Mater.* **2018**, *5*, 025002.
- [46] F. Zhu, W. Chen, Y. Xu, C. Gao, D. Guan, C. Liu, D. Qian, S.-C. Zhang, J. Jia, *Nat. Mater.* **2015**, *14*, 1020.
- [47] C.-Z. Xu, Y.-H. Chan, P. Chen, X. Wang, D. Flötotto, J. A. Hlevyack, G. Bian, S.-K. Mo, M.-Y. Chou, T.-C. Chiang, *Phys. Rev. B* **2018**, *97*, 035122.
- [48] J. Deng, B. Xia, X. Ma, H. Chen, H. Shan, X. Zhai, B. Li, A. Zhao, Y. Xu, W. Duan, S.-C. Zhang, B. Wang, J. G. Hou, *Nat. Mater.* **2018**, *17*, 1081.
- [49] J. Gou, L. Kong, H. Li, Q. Zhong, W. Li, P. Cheng, L. Chen, K. Wu, *Phys. Rev. Mater.* **2017**, *1*, 054004.
- [50] C.-Z. Xu, Y.-H. Chan, Y. Chen, P. Chen, X. Wang, C. Dejoie, M.-H. Wong, J. A.

- Hlevyack, H. Ryu, H.-Y. Kee, N. Tamura, M.-Y. Chou, Z. Hussain, S.-K. Mo, T.-C. Chiang, *Phys. Rev. Lett.* **2017**, *118*, 146402.
- [51] J. Yuhara, B. He, N. Matsunami, M. Nakatake, G. Le Lay, *Adv. Mater.* **2019**, *31*, 1901017.
- [52] L. Li, Y. Yu, G. J. Ye, Q. Ge, X. Ou, H. Wu, D. Feng, X. H. Chen, Y. Zhang, *Nat. Nanotechnol.* **2014**, *9*, 372.
- [53] H. Liu, A. T. Neal, Z. Zhu, Z. Luo, X. Xu, D. Tománek, P. D. Ye, *ACS Nano* **2014**, *8*, 4033.
- [54] M. Pumera, Z. Sofer, *Adv. Mater.* **2017**, *29*, 1605299.
- [55] A. J. Mannix, X.-F. Zhou, B. Kiraly, J. D. Wood, D. Alducin, B. D. Myers, X. Liu, B. L. Fisher, U. Santiago, J. R. Guest, M. J. Yacaman, A. Ponce, A. R. Oganov, M. C. Hersam, N. P. Guisinger, *Science* **2015**, *350*, 1513.
- [56] B. Feng, J. Zhang, Q. Zhong, W. Li, S. Li, H. Li, P. Cheng, S. Meng, L. Chen, K. Wu, *Nat. Chem.* **2016**, *8*, 563.
- [57] B. Feng, O. Sugino, R.-Y. Liu, J. Zhang, R. Yukawa, M. Kawamura, T. Iimori, H. Kim, Y. Hasegawa, H. Li, L. Chen, K. Wu, H. Kumigashira, F. Komori, T.-C. Chiang, S. Meng, I. Matsuda, *Phys. Rev. Lett.* **2017**, *118*, 096401.
- [58] S. Sheng, J.-B. Wu, X. Cong, Q. Zhong, W. Li, W. Hu, J. Gou, P. Cheng, P.-H. Tan, L. Chen, K. Wu, *ACS Nano* **2019**, *13*, 4133.
- [59] B. Kiraly, X. Liu, L. Wang, Z. Zhang, A. J. Mannix, B. L. Fisher, B. I. Yakobson, M. C. Hersam, N. P. Guisinger, *ACS Nano* **2019**, *13*, 3816.
- [60] R. Wu, I. K. Drozdov, S. Eltinge, P. Zahl, S. Ismail-Beigi, I. Božović, A. Gozar, *Nat. Nanotechnol.* **2019**, *14*, 44.
- [61] V. Kochat, A. Samanta, Y. Zhang, S. Bhowmick, P. Manimunda, S. A. S. Asif, A. S. Stender, R. Vajtai, A. K. Singh, C. S. Tiwary, P. M. Ajayan, *Sci. Adv.* **2018**, *4*, e1701373.

- [62] M.-L. Tao, Y.-B. Tu, K. Sun, Y.-L. Wang, Z.-B. Xie, L. Liu, M.-X. Shi, J.-Z. Wang, *2D Mater.* **2018**, *5*, 035009.
- [63] Z. Zhu, D. Tománek, *Phys. Rev. Lett.* **2014**, *112*, 176802.
- [64] E. Golias, M. Krivenkov, A. Varykhalov, J. Sánchez-Barriga, O. Rader, *Nano Lett.* **2018**, *18*, 6672.
- [65] J. Zhuang, C. Liu, Q. Gao, Y. Liu, H. Feng, X. Xu, J. Wang, J. Zhao, S. X. Dou, Z. Hu, Y. Du, *ACS Nano* **2018**, *12*, 5059.
- [66] W. Zhang, H. Enriquez, Y. Tong, A. Bendounan, A. Kara, A. P. Seitsonen, A. J. Mayne, G. Dujardin, H. Oughaddou, *Small* **2018**, *14*, 1804066.
- [67] J. L. Zhang, S. Zhao, C. Han, Z. Wang, S. Zhong, S. Sun, R. Guo, X. Zhou, C. D. Gu, K. Di Yuan, Z. Li, W. Chen, *Nano Lett.* **2016**, *16*, 4903.
- [68] J.-P. Xu, J.-Q. Zhang, H. Tian, H. Xu, W. Ho, M. Xie, *Phys. Rev. Mater.* **2017**, *1*, 061002.
- [69] C. Grazianetti, G. Faraone, C. Martella, E. Bonera, A. Molle, *Nanoscale* **2019**, DOI 10.1039/c9nr06037e.
- [70] P. Ares, F. Aguilar-Galindo, D. Rodríguez-San-Miguel, D. A. Aldave, S. Díaz-Tendero, M. Alcamí, F. Martín, J. Gómez-Herrero, F. Zamora, *Adv. Mater.* **2016**, DOI 10.1002/adma.201602128.
- [71] C. Gibaja, D. Rodríguez-San-Miguel, P. Ares, J. Gómez-Herrero, M. Varela, R. Gillen, J. Maultzsch, F. Hauke, A. Hirsch, G. Abellán, F. Zamora, *Angew. Chemie Int. Ed.* **2016**, DOI 10.1002/anie.201605298.
- [72] T. Lei, C. Liu, J.-L. Zhao, J.-M. Li, Y.-P. Li, J.-O. Wang, R. Wu, H.-J. Qian, H.-Q. Wang, K. Ibrahim, *J. Appl. Phys.* **2016**, *119*, 015302.
- [73] X. Wu, Y. Shao, H. Liu, Z. Feng, Y.-L. Wang, J.-T. Sun, C. Liu, J.-O. Wang, Z.-L. Liu, S.-Y. Zhu, Y.-Q. Wang, S.-X. Du, Y.-G. Shi, K. Ibrahim, H.-J. Gao, *Adv. Mater.* **2017**, *29*, 1605407.

- [74] M. Fortin-Deschênes, O. Waller, T. O. Menteş, A. Locatelli, S. Mukherjee, F. Genuzio, P. L. Levesque, A. Hébert, R. Martel, O. Moutanabbir, *Nano Lett.* **2017**, *17*, 4970.
- [75] Y. Shao, Z.-L. Liu, C. Cheng, X. Wu, H. Liu, C. Liu, J.-O. Wang, S.-Y. Zhu, Y.-Q. Wang, D.-X. Shi, K. Ibrahim, J.-T. Sun, Y.-L. Wang, H.-J. Gao, *Nano Lett.* **2018**, *18*, 2133.
- [76] T. Niu, W. Zhou, D. Zhou, X. Hu, S. Zhang, K. Zhang, M. Zhou, H. Fuchs, H. Zeng, *Adv. Mater.* **2019**, *31*, 1902606.
- [77] M. Jałochowski, M. Krawiec, *2D Mater.* **2019**, *6*, 045028.
- [78] X. Sun, Z. Lu, Y. Xiang, Y. Wang, J. Shi, G.-C. Wang, M. A. Washington, T.-M. Lu, *ACS Nano* **2018**, *12*, 6100.
- [79] J. Ji, X. Song, J. Liu, Z. Yan, C. Huo, S. Zhang, M. Su, L. Liao, W. Wang, Z. Ni, Y. Hao, H. Zeng, *Nat. Commun.* **2016**, *7*, 13352.
- [80] Z.-Q. Shi, H. Li, Q.-Q. Yuan, Y.-H. Song, Y.-Y. Lv, W. Shi, Z.-Y. Jia, L. Gao, Y.-B. Chen, W. Zhu, S.-C. Li, *Adv. Mater.* **2019**, *31*, 1806130.
- [81] K.-X. Chen, S.-S. Lyu, X.-M. Wang, Y.-X. Fu, Y. Heng, D.-C. Mo, *J. Phys. Chem. C* **2017**, *121*, 13035.
- [82] S. Zhang, W. Zhou, Y. Ma, J. Ji, B. Cai, S. A. Yang, Z. Zhu, Z. Chen, H. Zeng, *Nano Lett.* **2017**, *17*, 3434.
- [83] L. Lu, X. Tang, R. Cao, L. Wu, Z. Li, G. Jing, B. Dong, S. Lu, Y. Li, Y. Xiang, J. Li, D. Fan, H. Zhang, *Adv. Opt. Mater.* **2017**, *5*, 1700301.
- [84] M. Salinga, B. Kersting, I. Ronneberger, V. P. Jonnalagadda, X. T. Vu, M. Le Gallo, I. Giannopoulos, O. Cojocar-Mirédin, R. Mazzarello, A. Sebastian, *Nat. Mater.* **2018**, *17*, 681.
- [85] G. Pizzi, M. Gibertini, E. Dib, N. Marzari, G. Iannaccone, G. Fiori, *Nat. Commun.* **2016**, *7*, 12585.
- [86] J. Gu, Z. Du, C. Zhang, J. Ma, B. Li, S. Yang, *Adv. Energy Mater.* **2017**, *7*, 1700447.

- [87] C. Kamal, M. Ezawa, *Phys. Rev. B* **2015**, *91*, 085423.
- [88] H. Zhang, Y. Ma, Z. Chen, *Nanoscale* **2015**, *7*, 19152.
- [89] S. M. Beladi-Mousavi, A. M. Pourrahimi, Z. Sofer, M. Pumera, *Adv. Funct. Mater.* **2018**, *29*, 1807004.
- [90] C. L. Kane, E. J. Mele, *Phys. Rev. Lett.* **2005**, *95*, 226801.
- [91] F. Reis, G. Li, L. Dudy, M. Bauernfeind, S. Glass, W. Hanke, R. Thomale, J. Schäfer, R. Claessen, *Science* **2017**, *357*, 287.
- [92] Y. Du, G. Qiu, Y. Wang, M. Si, X. Xu, W. Wu, P. D. Ye, *Nano Lett.* **2017**, *17*, 3965.
- [93] J. Qin, G. Qiu, J. Jian, H. Zhou, L. Yang, A. Charnas, D. Y. Zemlyanov, C.-Y. Xu, X. Xu, W. Wu, H. Wang, P. D. Ye, *ACS Nano* **2017**, *11*, 10222.
- [94] Q. Wang, M. Safdar, K. Xu, M. Mirza, Z. Wang, J. He, *ACS Nano* **2014**, *8*, 7497.
- [95] Z. Xie, C. Xing, W. Huang, T. Fan, Z. Li, J. Zhao, Y. Xiang, Z. Guo, J. Li, Z. Yang, B. Dong, J. Qu, D. Fan, H. Zhang, *Adv. Funct. Mater.* **2018**, *28*, 1705833.
- [96] Y. Wang, G. Qiu, R. Wang, S. Huang, Q. Wang, Y. Liu, Y. Du, W. A. Goddard, M. J. Kim, X. Xu, P. D. Ye, W. Wu, *Nat. Electron.* **2018**, *1*, 228.
- [97] X. Huang, J. Guan, Z. Lin, B. Liu, S. Xing, W. Wang, J. Guo, *Nano Lett.* **2017**, *17*, 4619.
- [98] J.-H. Choi, P. Cui, W. Chen, J.-H. Cho, Z. Zhang, *Wiley Interdiscip. Rev. Comput. Mol. Sci.* **2017**, *7*, e1300.
- [99] P. Ranjan, T. K. Sahu, R. Bhushan, S. S. Yamijala, D. J. Late, P. Kumar, A. Vinu, *Adv. Mater.* **2019**, *31*, 1900353.
- [100] C. Grazianetti, E. Cinquanta, A. Molle, *2D Mater.* **2016**, *3*, 012001.
- [101] A. J. Mannix, B. Kiraly, M. C. Hersam, N. P. Guisinger, *Nat. Rev. Chem.* **2017**, *1*, 0014.
- [102] R. Friedlein, Y. Yamada-Takamura, *J. Phys. Condens. Matter* **2015**, *27*, 203201.
- [103] N. D. Drummond, V. Zólyomi, V. I. Fal'ko, *Phys. Rev. B* **2012**, *85*, 075423.

- [104] J. Qiu, H. Fu, Y. Xu, Q. Zhou, S. Meng, H. Li, L. Chen, K. Wu, *ACS Nano* **2015**, *9*, 11192.
- [105] P. Moras, T. O. Montes, P. M. Sheverdyayeva, A. Locatelli, C. Carbone, *J. Phys. Condens. Matter* **2014**, *26*, 185001.
- [106] C. Grazianetti, D. Chiappe, E. Cinquanta, M. Fanciulli, A. Molle, *J. Phys. Condens. Matter* **2015**, *27*, 255005.
- [107] E. Cinquanta, G. Fratesi, S. dal Conte, C. Grazianetti, F. Scotognella, S. Stagira, C. Vozzi, G. Onida, A. Molle, *Phys. Rev. B* **2015**, *92*, 165427.
- [108] Z. Qin, J. Pan, S. Lu, Y. Shao, Y. Wang, S. Du, H.-J. Gao, G. Cao, *Adv. Mater.* **2017**, *29*, 1606046.
- [109] A. W. Tsen, L. Brown, M. P. Levendorf, F. Ghahari, P. Y. Huang, R. W. Havener, C. S. Ruiz-Vargas, D. A. Muller, P. Kim, J. Park, *Science* **2012**, *336*, 1143.
- [110] X. Liu, Z. Zhang, L. Wang, B. I. Yakobson, M. C. Hersam, *Nat. Mater.* **2018**, *17*, 783.
- [111] H. Liu, H. Feng, Y. Du, J. Chen, K. Wu, J. Zhao, *2D Mater.* **2016**, *3*, 025034.
- [112] A. Molle, C. Grazianetti, D. Chiappe, E. Cinquanta, E. Cianci, G. Tallarida, M. Fanciulli, *Adv. Funct. Mater.* **2013**, *23*, 4340.
- [113] J. L. Zhang, S. Zhao, M. Telychko, S. Sun, X. Lian, J. Su, A. Tadich, D. Qi, J. Zhuang, Y. Zheng, Z. Ma, C. Gu, Z. Hu, Y. Du, J. Lu, Z. Li, W. Chen, *Nano Lett.* **2019**, *acs.nanolett.9b01796*.
- [114] E. Cinquanta, E. Scalise, D. Chiappe, C. Grazianetti, B. Van Den, *J. Phys. Chem. C* **2013**, *1*.
- [115] M. Amani, C. Tan, G. Zhang, C. Zhao, J. Bullock, X. Song, H. Kim, V. R. Shrestha, Y. Gao, K. B. Crozier, M. Scott, A. Javey, *ACS Nano* **2018**, *12*, 7253.
- [116] W. G. Vandenberghe, M. V. Fischetti, *Nat. Commun.* **2017**, *8*, 14184.
- [117] S. Tang, C. Zhang, D. Wong, Z. Pedramrazi, H.-Z. Tsai, C. Jia, B. Moritz, M. Claassen, H. Ryu, S. Kahn, J. Jiang, H. Yan, M. Hashimoto, D. Lu, R. G. Moore, C.-C.

Hwang, C. Hwang, Z. Hussain, Y. Chen, M. M. Ugeda, Z. Liu, X. Xie, T. P.

Devereaux, M. F. Crommie, S.-K. Mo, Z.-X. Shen, *Nat. Phys.* **2017**, *13*, 683.

[118] Z. Fei, T. Palomaki, S. Wu, W. Zhao, X. Cai, B. Sun, P. Nguyen, J. Finney, X. Xu, D. H. Cobden, *Nat. Phys.* **2017**, *13*, 677.

[119] M. Liao, Y. Zang, Z. Guan, H. Li, Y. Gong, K. Zhu, X.-P. Hu, D. Zhang, Y. Xu, Y.-Y. Wang, K. He, X.-C. Ma, S.-C. Zhang, Q.-K. Xue, *Nat. Phys.* **2018**, *14*, 344.

[120] C. Lin, W. Cheng, G. Chai, H. Zhang, *Phys. Chem. Chem. Phys.* **2018**, *20*, 24250.

[121] Z. Zhang, A. J. Mannix, Z. Hu, B. Kiraly, N. P. Guisinger, M. C. Hersam, B. I. Yakobson, *Nano Lett.* **2016**, *16*, 6622.

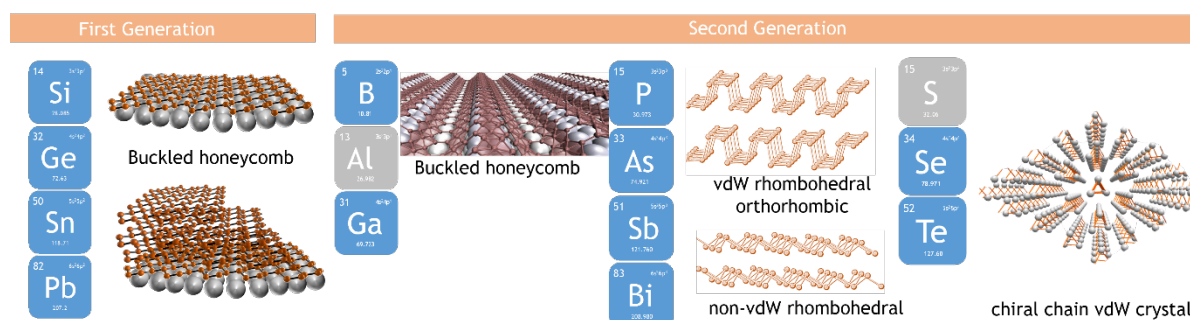


Figure 1. A general taxonomy of the first and second Xene generation grouped according to the periodic table and key structural properties. Blue symbols indicate the elements already reported in their Xene form, gray symbols are those (namely Al and S) not yet synthesized. The second generation lattice structures are reproduced with permission.^[54,115,121] Copyright Year, Publisher.

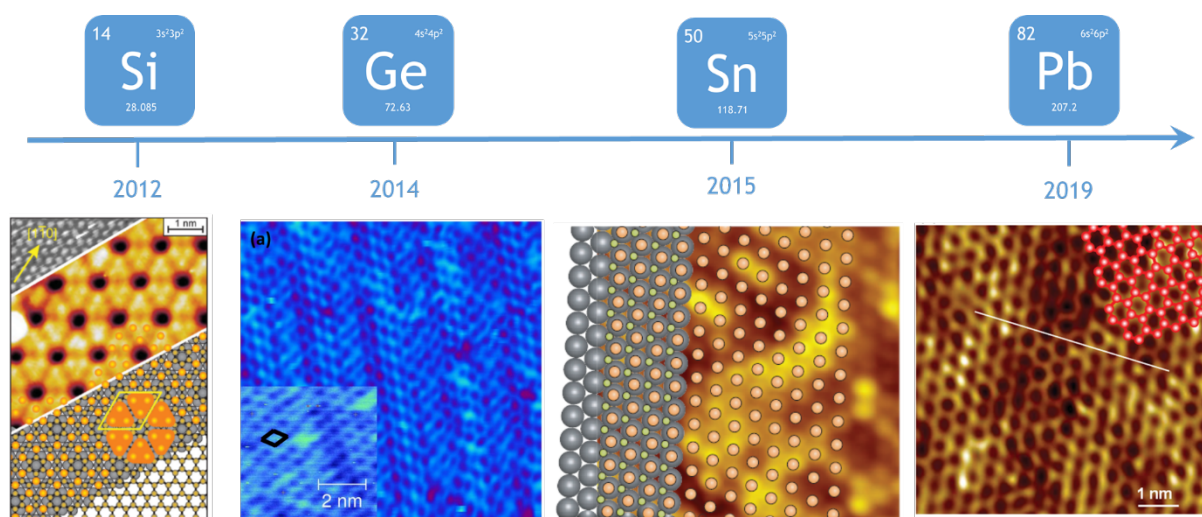


Figure 2. First generation Xenes: silicene, germanene, stanene, and plumbene obtained by the respective elements of the group 14 and year of their debut. Corresponding STM topographies showing the atomic structures of their lattice on supporting substrates like Ag(111) (silicene), Au(111) (germanene), $\text{Bi}_2\text{Te}_3(111)$ (stanene), and PbPd alloy (plumbene). Reproduced with permission.^[2,32,46,51] Copyright Year, Publisher.

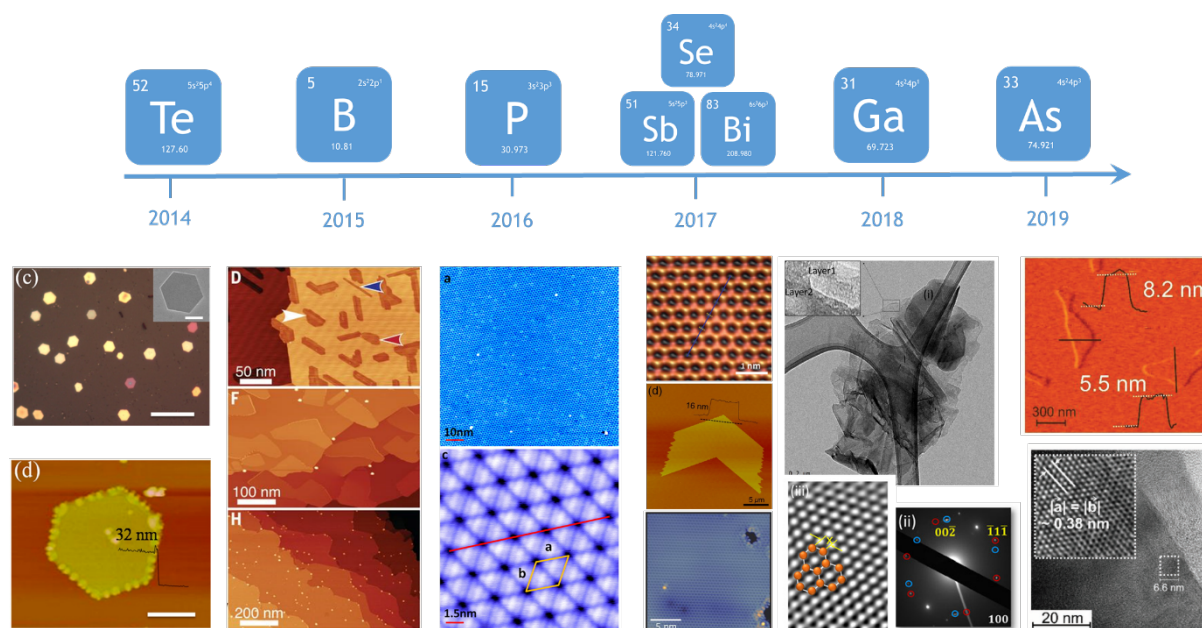


Figure 3. Second generation Xenes: tellurene, borophene, phosphorene, antimonene, selenene, bismuthene, gallenene, and arsenene obtained by the respective elements of the group 13, 15, and 16, and year of their debut. Corresponding topographies showing the Xene lattice on supporting substrates like mica (tellurene), Ag(111) (borophene), Au(111) (phosphorene), Ge(111) (antimonene), SiO_2/Si (selenene), $\text{SiC}(0001)$ (bismuthene), SiO_2 (gallenene), and mica (arsenene). Reproduced with permission.^[55,61,67,73,89,91,93,94] Copyright Year, Publisher.

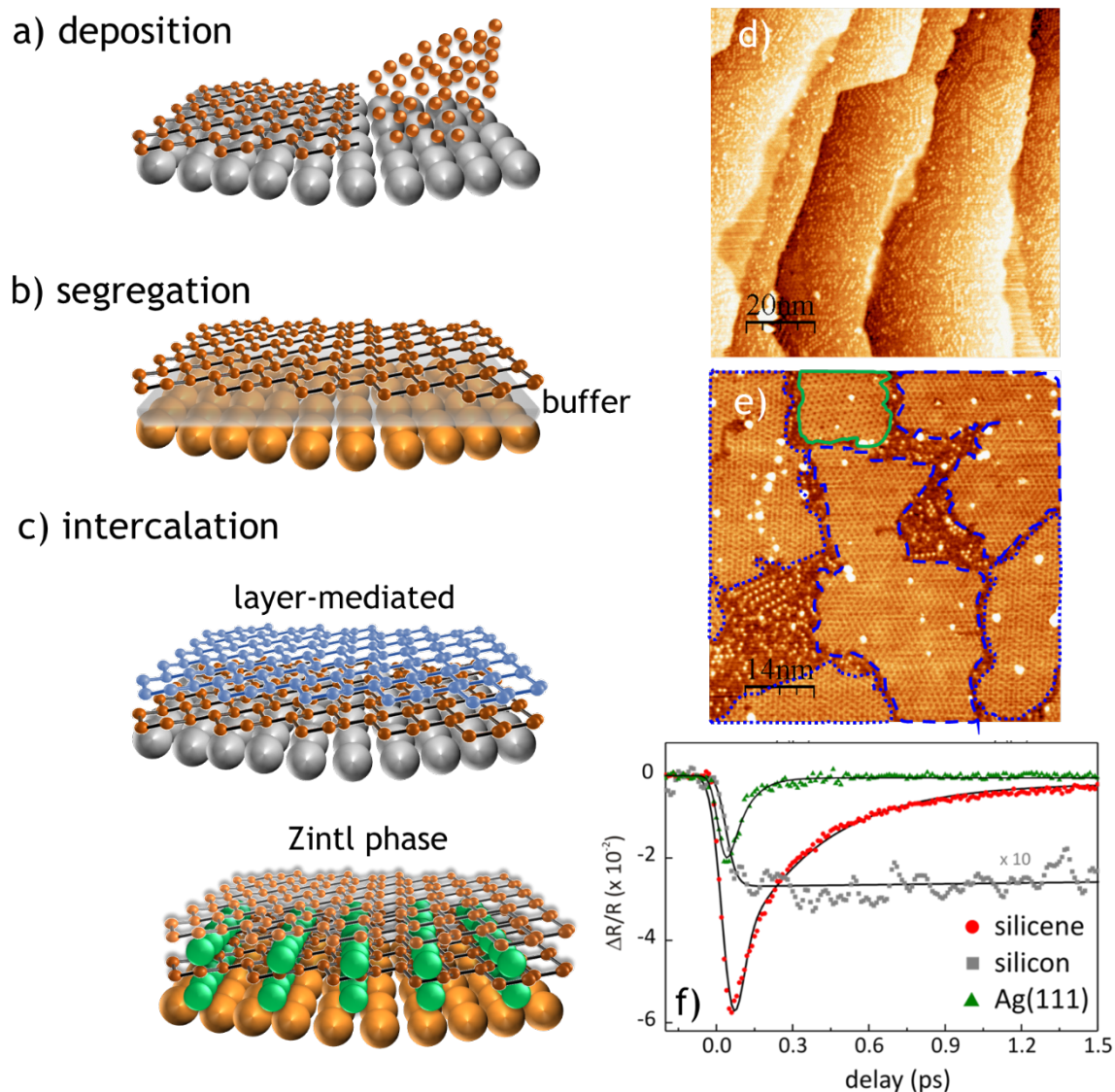


Figure 4. Schematic view of the epitaxial methodologies discussed in the text. a) epitaxy by deposition b) epitaxy by segregation c) epitaxy by intercalation via mediation of another 2D layer (top) or through the formation of Zintl phase compound. The two growth regimes of silicene on Ag(111) as a function of the deposition time. d) nucleation of silicene seeds in a sub-monolayer regime and e) formation of the 2D structured domains. Reproduced with permission.^[106] Copyright Year, Publisher. f) Comparative carrier dynamics study of silicene-on-Ag(111), bulk silicon and lone Ag(111). The silicene-substrate system shows an overall metallic character due to the coupling of the Xene with the substrate. Reproduced with permission.^[107] Copyright Year, Publisher.

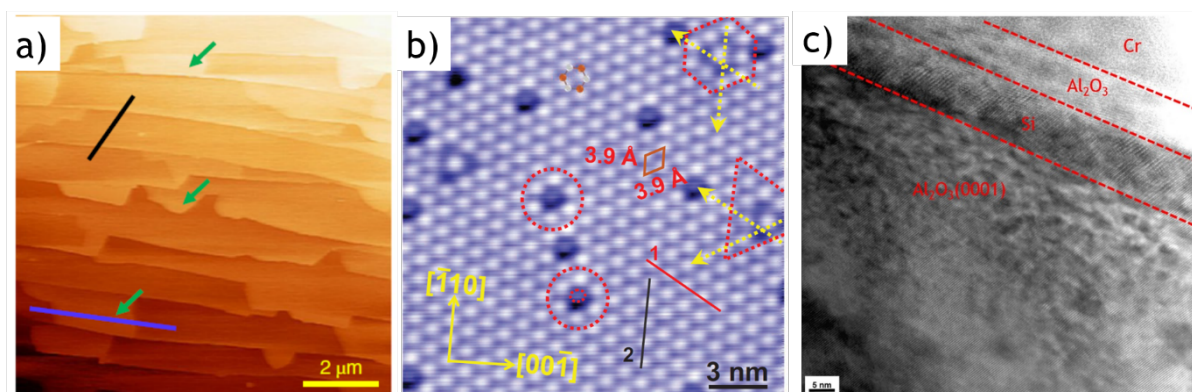


Figure 5. Three paradigmatic examples respectively showing the scalability, quality, and stability items discussed in main text. a) large-area STM image showing epitaxial growth of borophene on Cu(111) surface. b) STM study of defects on the antimonene on Cu(111) surface. c) Cross-section view by transmission electron microscopy showing the stability of silicene (grown on c-Al₂O₃ substrate) provided through amorphous Al₂O₃ capping layer. Reproduced with permission.^[21,60,76] Copyright Year, Publisher.

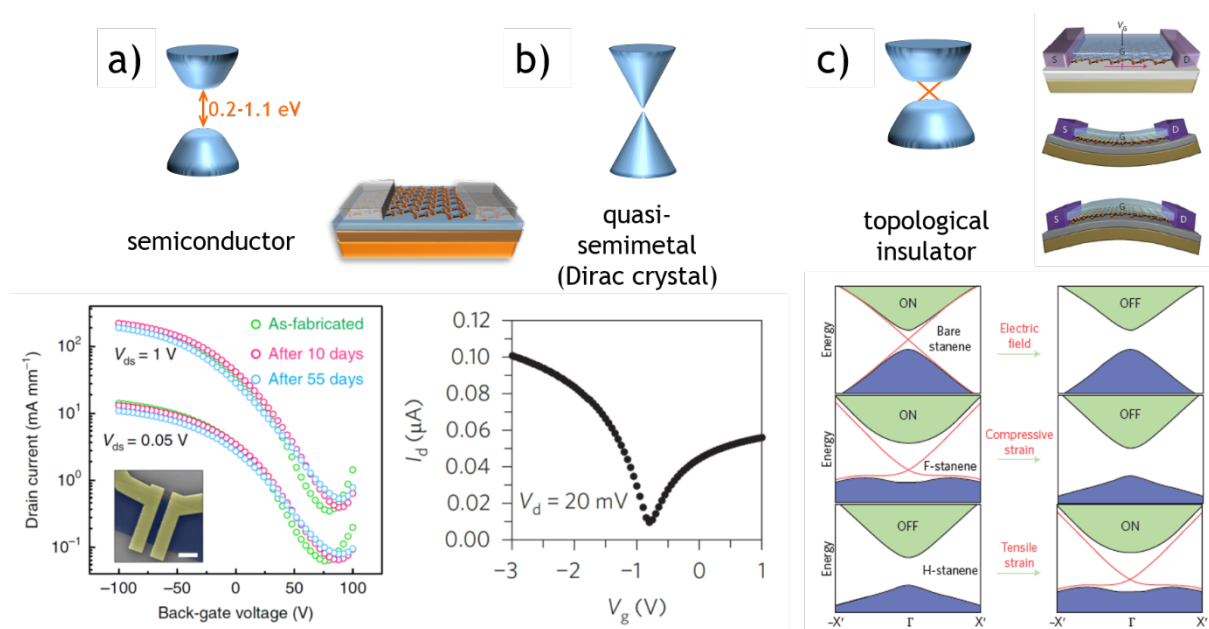


Figure 6. Schematic band structure diagram of a) semiconductor Xenes and their range of bandgap values. In the plot, the characteristic transfer curves of a tellurene-based FET and the stability of the device performance in ambient condition up to 55 days. Reproduced with permission.^[96] Copyright Year, Publisher. b) Xene with Dirac-like band dispersion showing a quasi-semimetallic character. In the plot, the ambipolar transport characteristic of a silicene-based FET operating at room temperature. Reproduced with permission.^[3] Copyright Year, Publisher. c) Band structure diagram and edge-states emerging in the gap (orange lines) of a Xene showing topological insulator features. The case of stanene and the topological phase transitions induced by an out-of-plane electric field, compressive and tensile strain is shown in the graphs. The envisioned integration of a 2D topological insulator into a flexible FET (TI-FET) is shown. Reproduced with permission.^[7] Copyright Year, Publisher.

The novel class of mono-elemental two-dimensional materials is reviewed and classified into two generations of Xenes. The attention is turned on the epitaxial methodologies for their synthesis and on the key-points, like scalability, quality, and stability, which enable the Xenes exploitation in a wealth of technological applications including the integration into ultra-scaled functional devices.

Keyword: Xenes, two-dimensional, post-graphene, epitaxy, atomically thin

C. Grazianetti, C. Martella, and A. Molle*

The Xenes Generations: a taxonomy of epitaxial single-element two-dimensional materials

